
Controlling cell interactions by micropatterning in co-cultures: Hepatocytes and 3T3 fibroblasts

Sangeeta N. Bhatia,[†] Martin L. Yarmush, and Mehmet Toner*

Center for Engineering in Medicine, Surgical Services, Massachusetts General Hospital, Shriners Burns Institute, and Department of Surgery, Harvard Medical School, Boston, Massachusetts

The repair or replacement of damaged tissues using *in vitro* strategies has focused on manipulation of the cell environment by modulation of cell–extracellular matrix interactions, cell–cell interactions, or soluble stimuli. Many of these environmental influences are easily controlled using macroscopic techniques; however, in co-culture systems with two or more cell types, cell–cell interactions have been difficult to manipulate precisely using similar methods. Although microfabrication has been widely utilized for the spatial control of cells in culture, these methods have never been adapted to the simultaneous co-cultivation of more than one cell type. We have developed a versatile technique for micropatterning of

two different cell types based on existing strategies for surface modification with aminosilanes linked to biomolecules and the manipulation of serum content of cell culture media. This co-culture technique allowed manipulation of the initial cellular microenvironment without variation of cell number. Specifically, we were able to control the level of homotypic interaction in cultures of a single cell type and the degree of heterotypic contact in co-cultures over a wide range. This methodology has potential applications in tissue engineering, implant biology, and developmental biology, both in the arena of basic science and optimization of function for technological applications. © 1997 John Wiley & Sons, Inc.

INTRODUCTION

The repair or replacement of damaged tissues using *in vitro* strategies has focused on manipulation of the cell environment by modulation of cell–extracellular matrix interactions, cell–cell interactions, or soluble stimuli. Development of functional tissue substitutes through “tissue engineering” has been facilitated by the ability to control each of these environmental influences. However, in co-culture systems with two or more cell types, cell–cell interactions have been difficult to manipulate precisely. These interactions are important in normal physiology of many organ systems including vasculature (smooth muscle cell and endothelium),¹ skeletal muscle (myocyte and peripheral nerve),² and liver (hepatocyte and sinusoidal endothelium).³ In addition these interactions are implicated in the pathophysiology of certain diseases: atherosclerosis in cardiovascular disease,⁴ denervation atrophy in skeletal muscle,⁵ and alcoholic cirrhosis in liver dis-

ease.⁶ Lastly, many of these interactions also are involved in development where differentiation cues are obtained by contact or proximity to another cell type.

Traditional co-culture systems have assessed the influence of nonparenchymal cell populations on parenchymal cells by variations in cell-seeding density or addition of excised tissue or confluent coverslips to existing cultures. Alternatively, physical separation of cell cultures through use of conditioned media^{7,8} or porous filter inserts⁹ has been utilized. In addition dynamic cell–cell interaction has been studied in monolayers of a primary cell type in the presence of a shearing fluid containing a secondary cell type.^{10,11} One limitation of these co-culture systems is the inability to vary local cell-seeding density independently of the cell number. Micropatterning technology, or the ability to spatially control cell placement at the single-cell level, will allow us to precisely manipulate cell–cell interactions of interest.

Microfabrication techniques have been widely utilized for the spatial control of cells in culture.^{12–21} Many strategies have employed variations in charge,^{22,23} hydrophilicity,^{17,24} and topology^{17,25,26} to mediate selective adhesion of one cell type by differential serum-protein adsorption, or variations in surface free energy. In addition specific use of biomolecules alone,^{12,27} or in conjunction with aminosilanes^{16,19} or self-assembled mono-

*To whom correspondence should be addressed at Shriners Research Center, One Kendall Square, 1400W, Cambridge, MA 02139.

[†]S. N. Bhatia is a graduate student at Harvard-MIT, Division of Health Sciences and Technology, Cambridge, Massachusetts

layers²⁸ have been used to micropattern cells. A variety of cell types have been examined with micropatterning techniques such as neuroblastoma cells,²⁴ BHK epithelial cells,¹⁷ hepatocytes,^{28–30} and myocytes¹⁵ with spatial resolution on the micron scale. These studies examined a wide array of physiologic functions such as neuronal growth cone guidance, effects of cell shape on function, and electrical coupling through gap junctions. However, these methods have never been adapted to the simultaneous co-cultivation of more than one cell type.

In this study we describe an adaptable method for generating two-dimensional, anisotropic, model surfaces capable of organizing a single cell type or two different cell types in discrete spatial locations. We have chosen a primary rat hepatocyte/3T3 fibroblast cell system because of its potential significance in both basic science and technology development and based on widely reported interactions observed in this co-culture model.^{7,8,31–34} We have used photolithography to pattern biomolecules on glass substrates which mediate cell adhesion of the first cell type, hepatocytes. The second cell type, 3T3 fibroblasts, undergoes non-specific, serum-mediated attachment to the remaining unmodified areas. Here we describe the specifics of our methodology and discuss its facility and versatility as compared with other existing micropatterning techniques.

MATERIALS AND METHODS

Microfabrication techniques were used to modify glass substrates with biomolecules. These modified substrates were utilized to pattern a single cell type or micropattern co-cultures in various configurations. Figure 1 schematically depicts the overall process for one representative pattern.

Microfabrication of substrates

The experimental substrates were produced utilizing standard microfabrication techniques at Microsystems Technology Lab, MIT, Cambridge, Massachusetts. Chrome masks of the desired dimensions were generated on a pattern generator (Gyrex) which transferred the pattern to a chromium-coated quartz plate using a contact printer and a developer. Round, 2-in. diameter \times 0.02-in. thick borosilicate wafers (Erie Scientific, Portsmouth, NH) were cleaned in a piranha solution (3:1 H₂SO₄; 30% H₂O₂) for 10 min, rinsed, and blown dry with a N₂ gun. Wafers were then dehydrated by baking for 60 min at 200°C. Discs were subsequently coated with positive photoresist (OCG 820-27 centistokes) on a Headway spin-coater with vacuum chuck as follows: dispense photoresist at 500 rpm for

2 s, spread photoresist at 750 rpm for 6 s, spin at 4000 rpm for 30 s, resulting in a 1- μ m coating (step A, Fig. 1). Wafers were then prebaked for 5 min at 90°C to remove residual solvent and anneal any stress in the film. Wafers were exposed in a Bottom Side Mask Aligner (Karl Suss, Waterbury Center, VT) to ultraviolet light through the desired chromium mask to create a latent image in the resist layer. Exposure occurred under vacuum-enhanced contact for 3 s. Exposed photoresist was then developed to produce the final three-dimensional relief image for 70 s in developer (OCG 934 1:1), rinsed three times under running deionized water and cascade-rinsed for 2 min (step B, Fig. 1). Subsequently, discs were hard-baked for 30 min at 120°C to remove residual developing solvents and promote adhesion of the film. Finally, substrates were exposed to oxygen plasma at 250 W for 4 min to remove unwanted resist in areas to be subsequently modified. Wafers were stored at room temperature for up to 2 months. Substrates were subsequently re-exposed to oxygen plasma 24 h prior to further processing to ensure availability of borosilicate for surface modification on a Plasma Day Etcher at a base vacuum of 50 mTorr and O₂ pressure of 100 mTorr at a power of 100 W for 2–4 min.

Surface modification of substrates

Substrates were modified using experimental methods similar to those developed by Lom et al.¹⁹ and Britland et al.¹⁶ (step C, Fig. 1). Briefly, substrates were rinsed two times in distilled, deionized (DD) water and allowed to air dry. Silane immobilization onto exposed glass was performed by immersing samples for 30 s in freshly prepared, 2% v/v solution of 3-[(2-aminoethyl) amino] propyltrimethoxysilane (AS, Hüls America, Piscataway, NJ) in water followed by two rinses in 200 mL DD water. Wafers were then dried with nitrogen gas and baked at 120°C for 10 min. Next, discs were immersed in 20 mL of 2.5% v/v solution of glutaraldehyde in phosphate-buffered saline (PBS) (pH 7.4) for 1 h at 25°C. Substrates were then rinsed twice in fresh PBS, and immersed in a 4-mL solution of a 1:1 solution of 1 mg/mL collagen I (preparation described in detail elsewhere)³⁵; DD water for 15 min at 25°C. Discs were subsequently immersed in acetone and placed in a bath sonicator (Bransonic) for 15 min to remove residual photoresist ultrasonically (step D, Fig. 1). Wafers were then rinsed twice in DD water, and soaked overnight in 70% ethanol for sterilization (step E, Fig. 1).

Surface Characterization of Substrates

Autofluorescence

Wafers were observed using a Nikon Diaphot (Garden City, NY) microscope equipped with a Hg lamp

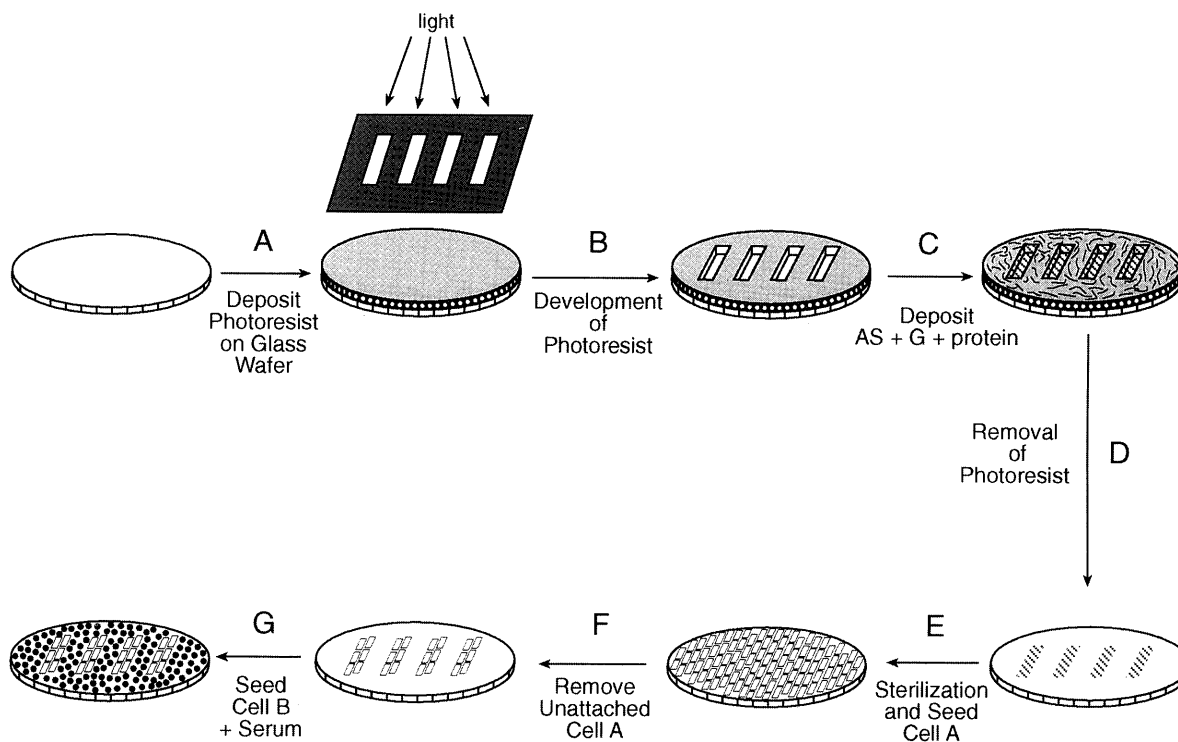


Figure 1. Schematic of process to generate micropattern co-cultures. Borosilicate wafers were spin-coated with positive photoresist (step A) and exposed to ultraviolet light through a chromium mask. Exposed photoresist was then solubilized in developer solution, resulting in a glass/photoresist pattern (step B). Subsequently, aminoethylaminopropyltrimethoxysilane (AS), glutaraldehyde (G), and a protein were bound to the surface of the wafer (step C). Photoresist was then lifted off by sonication in acetone resulting in a glass/protein pattern (step D). After sterilization in 70% ethanol, wafers were incubated with a suspension of cell type A in serum-free media (step E) and washed with media (step F) resulting in a glass/cell A pattern. Lastly, surfaces were incubated with a suspension of cell type B in serum-containing media, thereby allowing attachment to unmodified regions of the substrate (step G).

and power supply. The autofluorescence of photoresist (excitation 550 nm, emission 575 nm) was used to visualize micropatterned substrates prior to surface modification. Absence of autofluorescence after sonication was taken to verify removal.

Profilometry

Profilometry was performed to characterize surface topology at the Center for Material Science Engineering (CMSE) on a Dektak 3 Profilometer (Veeco Instruments) with a 12.5- μm radius probe at a scan rate of 100 $\mu\text{m/s}$.

Atomic force microscopy

Atomic force microscopy (AFM) was performed in order to characterize the spatial distribution of immobilized groups at the CMSE, MIT, on a Nanoscope 3 (Digital Instruments) equipped with a standard 117- μm silicon cantilever operating in tapping mode with a scan size of 100 μm .

Indirect immunofluorescence of collagen I

Collagen-derivatized substrates were incubated at 37°C with undiluted rabbit anti-rat collagen I antisera

(Biosciences), by inverting substrates onto parafilm which contained a droplet of (50 μL) of antisera for 1 h. Substrates were then washed thoroughly in PBS and placed on a rotating shaker at 25°C for 30 min. This washing procedure was repeated twice. Next, discs were inverted onto parafilm with 50 μL (1:20) of dichlorotriazinylamino fluorescein (DTAF)-conjugated donkey anti-rabbit IgG (Jackson Laboratories, West Grove, PA) in blocking solution. Blocking solution consisted of 3% w/w bovine serum albumin, 1% donkey serum, 0.04% sodium azide, pH 7.4. Finally, substrates were washed in PBS overnight, and observed by fluorescence microscopy (excitation 470 nm, emission 510 nm).

Cell culture

Hepatocyte isolation and culture

Hepatocytes were isolated from 2- to 3-month-old adult female Lewis rats (Charles River Laboratories, Wilmington, MA) weighing 180–200 g, by a modified procedure of Seglen.³⁶ Detailed procedures for isolation and purification of hepatocytes were previously de-

scribed by Dunn et al.³⁷ Routinely, 200–300 million cells were isolated with viability between 85% and 95%, as judged by trypan blue exclusion. Nonparenchymal cells, as judged by their size ($<10\ \mu\text{m}$ in diameter) and morphology (nonpolygonal or stellate), were less than 1%. Culture medium was Dulbecco's modified eagle's medium (DMEM, Gibco) supplemented with 10% fetal bovine serum (FBS, Sigma, St. Louis, MO), 0.5 U/mL insulin, 7 ng/mL glucagon, 20 ng/mL epidermal growth factor, 7.5 $\mu\text{g}/\text{mL}$ hydrocortisone, 200 U/mL penicillin, 200 $\mu\text{g}/\text{mL}$ streptomycin, and 50 $\mu\text{g}/\text{mL}$ gentamycin. Serum-free culture medium was identical except for the inclusion of 40 $\mu\text{g}/\text{mL}$ of L-proline (Sigma, St. Louis, MO) and exclusion of FBS.³⁸

NIH 3T3-J2 Culture

NIH 3T3-J2 cells were the gift of Howard Green, Harvard Medical School. Cells grown to confluence were trypsinized in 0.01% trypsin (ICN Biomedicals, Costa Mesa, CA)/0.01% EDTA (Boehringer Mannheim, Indianapolis, IN) solution in PBS for 5 min and then resuspended in 25 mL media. Approximately 10% of the cells were inoculated into a fresh tissue culture flask. Cells were passaged at confluency no more than 12 times. Cells were cultured in 75 cm^2 flasks (Fisher, Springfield, NJ) at 10% CO_2 , balance moist air. Culture medium consisted of DMEM (Gibco, Grand Island, NY) with high glucose, supplemented with 10% bovine calf serum (BCS, JRH Biosciences, Lenexa, KS) and 200 U/mL penicillin and 200 $\mu\text{g}/\text{mL}$ streptomycin.

Cell culture on modified surfaces

Wafers were rinsed in sterile water and incubated in 0.05% w/w bovine serum albumin (BSA) in water at 37°C for 1 h to precoat substrates with a nonadhesive protein. Substrates were then washed twice with serum-free media. Next, hepatocytes were seeded at high density ($4 \times 10^6/\text{mL}$) in serum-free media for 1.5 h at 37°C, 10% CO_2 , balance air (step E, Fig. 1). Surfaces were then rinsed twice by pipetting and then aspirating 4 mL of serum-free media, reseeded with hepatocytes for 1.5 h, rinsed with 4 mL of serum-free media, and incubated overnight (step F, Fig. 1). The following day 3T3 cells were trypsinized as described above, counted with a hemocytometer, and plated at $1 \times 10^6/\text{mL}$ in 2 mL of serum-containing, high-glucose DMEM, and allowed to attach overnight (step G, Fig. 1). Randomly distributed co-cultures consisted of hepatocyte seeding in the desired number (usually 250,000) on a uniformly collagen-derivatized surface, followed by 3T3 seeding after 24 h.

Immunofluorescent staining

Cultures were washed twice with 2 mL PBS, fixed and permeabilized with 10 mL of acetone at -20°C for 2 min,

and washed twice in 10 mL PBS. Cultures on wafers were incubated at 37°C with undiluted rabbit anti-rat pan cytokeratin antisera (Accurate Chemical, Westbury, PA) by inverting substrates onto parafilm containing a 50- μL droplet of antisera for 1 h. Substrates were then washed, incubated with secondary antibody, and washed as described above (see "Indirect immunofluorescence of collagen"). Secondary antibody also included rhodamine phalloidin (1:100, Molecular Probes, Eugene, OR) for fluorescent labeling of F-actin. Specimens were observed and recorded using a Nikon Diaphot microscope equipped with a Hg lamp and power supply, light-shuttering system (Uniblitz D122), CCD camera (Optitronics CCD V1470), and MetaMorph Image Analysis System (Universal Imaging, Westchester, PA) for digital image acquisition.

Image analysis

To quantitatively describe the extent of heterotypic interactions, we measured the fraction of cell perimeter in contact with adjacent cells of a different cell type (χ). For example, $\chi = 1$ for a single cell island whereas $\chi = 0$ for a cell amidst hepatocyte neighbors. Images were acquired as described above and analyzed with MetaMorph Image Analysis System. Cells were sampled from each field and manually outlined to obtain individual cell perimeters, P . Subsequently, the regions of heterotypic cell-cell contact were similarly delineated, F . Each cell was assigned its characteristic $\chi = F/P$ and these values of χ were averaged over 20–50 cells for each condition.

RESULTS

The methodology presented here represents significant modification of many existing techniques. Therefore we initially performed surface characterization studies on substrates in the absence of cells to validate our ability to obtain spatially defined surface chemistries. Subsequently the ability to micropattern single-cell cultures and co-cultures including two different cell types was investigated.

Surface characterization

Topological and spatial uniformities of photoresist patterns were assessed using profilometry and autofluorescent properties of photoresist. The photoresist coating was found to be approximately 1.35 μm in thickness using the specified spin-coating parameters [see Fig. 2(B)]. Furthermore, the thickness of photoresist varied $<5\%$ within each scan. Autofluorescence of photoresist was utilized to examine integrity and

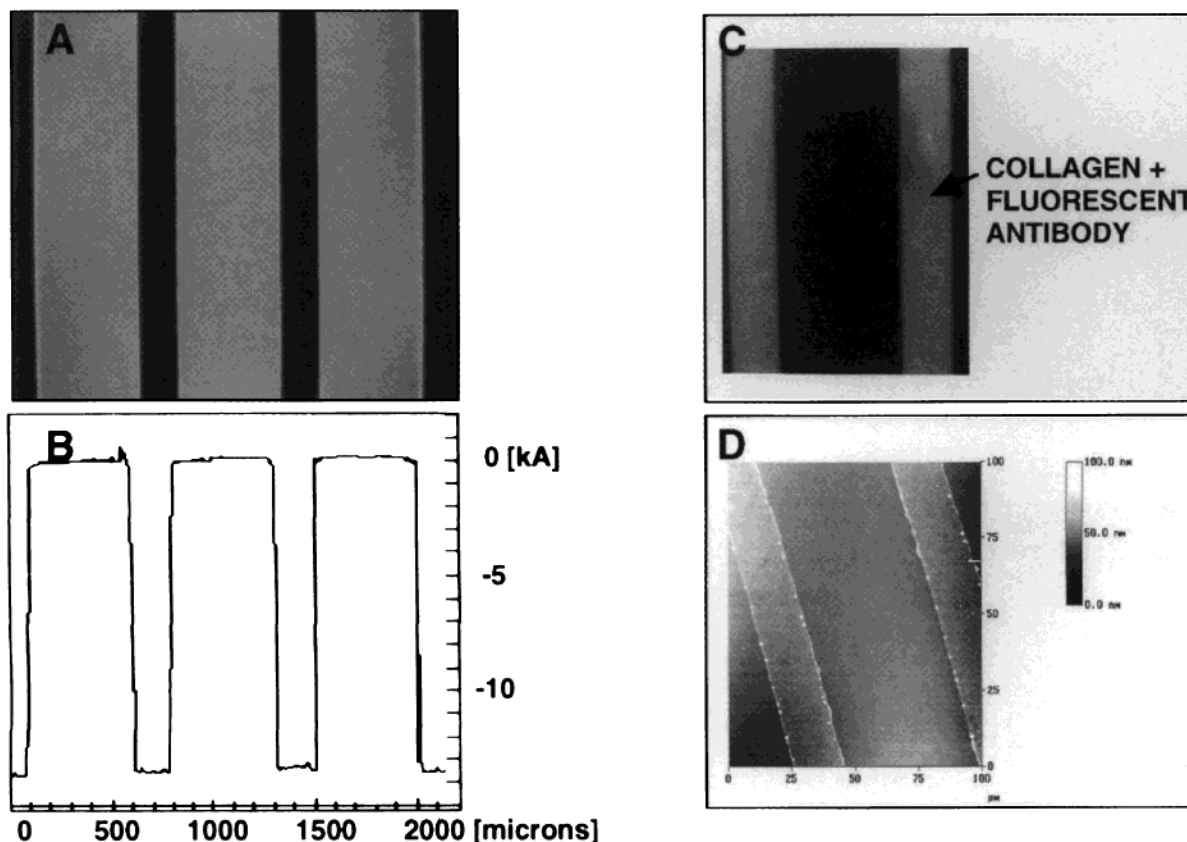


Figure 2. Surface characterization. (A) Fluorescent micrograph of autofluorescent photoresist pattern of $500\ \mu\text{m}$ width with intervening lanes of bare glass of $200\ \mu\text{m}$. Excitation $550\ \text{nm}$, emission $575\ \text{nm}$. (B) Profilometry scan of surface of photoresist pattern demonstrating approximately $1.35\ \mu\text{m}$ thickness of photoresist at specified coating parameters (see METHODS). Raised areas correspond with autofluorescent photoresist in panel A. (C) Fluorescent micrograph of indirect immunofluorescent stain of collagen I immobilized on surface demonstrating uniformity and high degree of spatial resolution corresponding to original photoresist pattern. (D) Atomic force micrograph of $50\text{-}\mu\text{m}$ lanes of borosilicate alternating with $20\text{-}\mu\text{m}$ lanes of collagen-modified glass. Average height of collagen lanes was $4\ \text{nm}$.

distribution of photoresist prior to and during processing. Figure 2(A, B) demonstrate autofluorescent regions corresponding to $\sim 1\ \mu\text{m}$ variations in thickness. Absence of any contaminant fluorescence in the dark lanes indicates complete, uniform removal of exposed photoresist during development.

Collagen immobilization via glutaraldehyde derivatization of patterned aminoethylaminopropyltrimethoxysilane (AS) surfaces was also characterized. The fluorescence micrographs in Figure 2(C) show the results of indirect immunofluorescent staining of areas of presumed collagen immobilization. Fluorescent regions, corresponding to regions of collagen localization, were patterned uniformly with spatial resolution on the micron level. Furthermore, fluorescent patterns corresponded to initial photoresist patterns without evidence of undercutting. More importantly, despite processing in acetone and 70% ethanol, collagen retained sufficient immunoreactivity for antibody binding.

Collagen-derivatized surfaces were also analyzed with AFM [Fig. 2(D)] to determine differences in topol-

ogy between unmodified and modified borosilicate. Modified regions with a width of $20\ \mu\text{m}$ were found to have an average height of $4\ \text{nm}$ above the unmodified, $50\text{-}\mu\text{m}$ lanes. These data can be utilized to approximate the number of collagen monolayers atop AS.

Micropatterning of co-cultures

Given the ability to reproducibly utilize photoresist patterns to generate immobilized collagen patterns, the applicability of these techniques to cellular micropatterning was examined. Seeding of the first cell type, hepatocytes, resulted in localization to collagen-derivatized regions and normal polygonal morphology. The cellular configurations were dictated by the positioning of collagen on glass, which was in turn controlled by the choice of chromium mask in the microfabrication procedure [Fig. 3(A,B)]. Furthermore, hepatocytes conformed to the edges of the collagen pattern on the modified glass. Typical hepatocyte diameter in suspension is $20\ \mu\text{m}$, whereas upon attach-

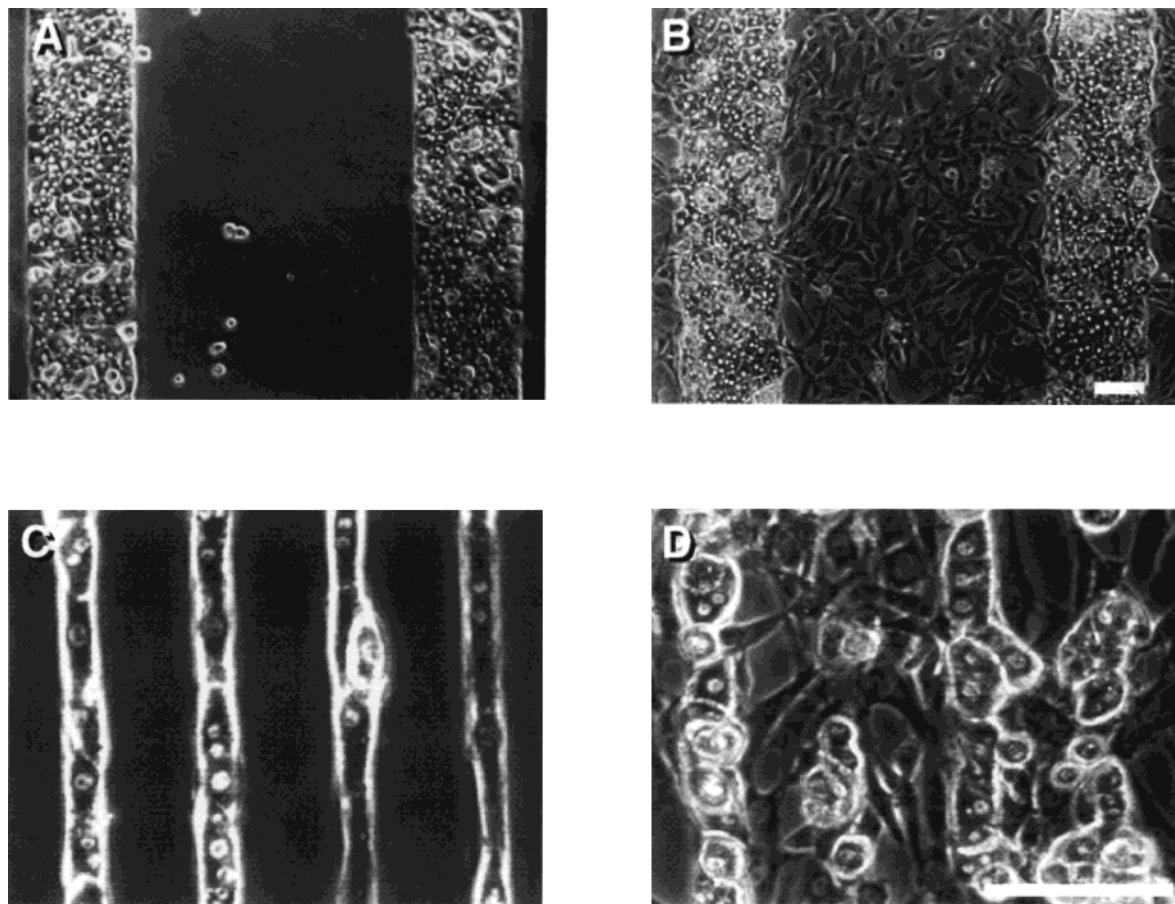


Figure 3. Phase-contrast micrographs of micropatterned hepatocytes and co-cultures with 3T3 fibroblasts. (A) Hepatocytes attached to 200- μm lanes of collagen-derivatized glass (250,000 per dish). (B) Hepatocytes attached to 200- μm lanes of collagen-derivatized glass (250,000 per dish) with fibroblasts attached to intervening, 500- μm glass lanes (2 million per dish). Photograph was taken 48 h after hepatocyte seeding, 24 h after fibroblast seeding. Scale bar corresponds to 100 μm . (C) Hepatocytes attached to 20 μm lanes of collagen-derivatized glass. Cells elongate in axial direction upon spreading (250,000 per dish). (D) Hepatocytes attached to 20- μm lanes of collagen-derivatized glass with fibroblasts attached to intervening, 50- μm glass lanes (2 million per dish). Photograph was taken 30 h after hepatocyte seeding, 6 h after fibroblast seeding. Scale bar corresponds to 100 μm .

ment and unconstrained spreading, cell diameters increase to 30–40 μm . Therefore, after attachment to 20- μm lanes, cells were observed to elongate in the axial direction upon spreading [Fig. 3(C)]. Similar cytoskeletal changes were observed in cells on corners of larger patterns or on the perimeter of circular patterns.

The versatility of this technique is seen in four representative phase-contrast micrographs in Figure 3. Initial hepatocyte patterns of 20 μm [Fig. 3(C)] and 200 μm [Fig. 3(A)] were modified by the addition of fibroblasts in serum-containing media. Fibroblasts were observed to localize solely to unmodified (glass) regions of patterned substrates resulting in micropatterned co-cultures of 20 $\mu\text{m}/50 \mu\text{m}$ [Fig. 3(D)] and 200 $\mu\text{m}/500 \mu\text{m}$ [Fig. 3(B)]. The grating pattern utilized was chosen for its illustrative potential; however, in principle, co-cultures can be achieved in any desired configuration. Thus, our approach is clearly adaptable to both micropatterning of single-cell cultures and co-cultures of two different cell types.

Spreading of the primary cell type typically resulted in negligible residual sites of collagen derivatization. Therefore, attachment of the secondary cell type would theoretically be limited either to unmodified glass or the surface of the primary cell type. In a separate set of studies, we determined that 3T3 fibroblasts do not undergo significant attachment to hepatocyte surfaces by performing plating experiments of fibroblasts on monolayers of hepatocytes which showed no attachment even after a 4-h incubation (data not shown). In addition, fibroblast attachment and spreading on glass was characterized by seeding cells in serum-containing media on glass coverslips where they were observed to attach and spread with high efficiency within 4 h (data not shown).

Indirect immunofluorescence was utilized to selectively stain cell populations and aid in visual discrimination between different cell types. Figure 4 compares presence of cytokeratin [Fig. 4 (A,B)], an intermediate filament expressed in hepatocytes but absent in mesen-

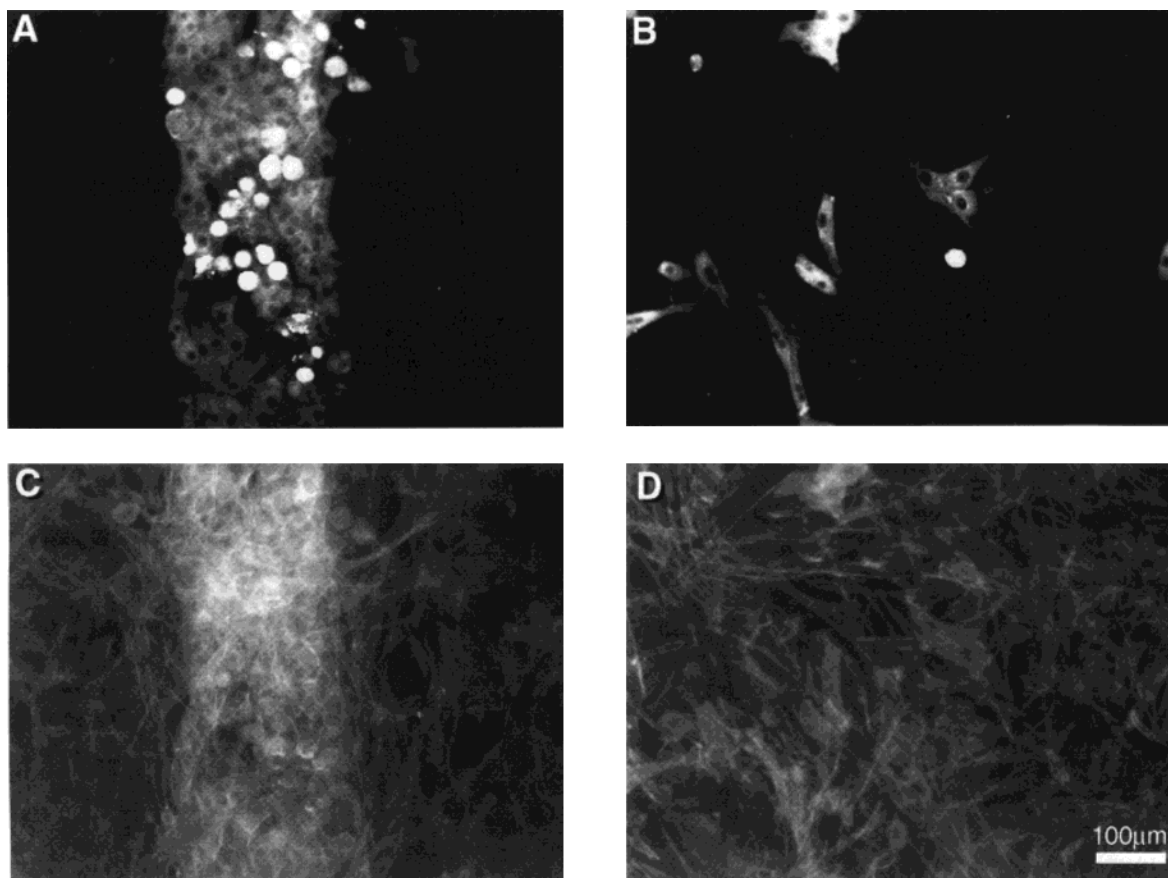


Figure 4. Immunofluorescent staining of micropattern co-cultures. Micrograph of indirect immunofluorescence of cytokeratin in micropatterned (A) and randomly distributed (B) co-cultures. The degree of homotypic hepatocyte interaction is significantly greater in A than B despite identical cell numbers in each subpopulation. F-Actin localization in micropatterned (C) and randomly distributed (D) co-cultures.

chymal cells, to F-actin [Fig. 4 (C,D)], a cytoskeletal protein present in all mammalian cells. The figure also contains a comparison of a patterned co-culture of $200\ \mu\text{m}/500\ \mu\text{m}$ [Fig. 4 (A,C)] compared with a randomly distributed (see METHODS) co-culture [Fig. 4 (B,D)] with identical, attached cell numbers of both cell populations. Of note is the level of homotypic hepatocyte interaction in Figure 4(A), a $200\text{-}\mu\text{m}$ stripe, versus Figure 4(B), a random distribution of cells. Hepatocytes in Figure 4(A) had primarily homotypic contacts, whereas those in Figure 4 (B) had predominantly heterotypic contacts. Furthermore, the distribution of heterotypic interaction over a patterned cell population is observed to be greatly reduced compared with random co-cultures where hepatocytes are shown to be present in single-cell islands, doublets, and triplets [Fig. 4(B)].

To quantitatively describe the extent of heterotypic contact, we used image analysis and perimeter tracing to define the fractional cell perimeter engaged in heterotypic cell contact as χ (see METHODS). Figure 5 schematically depicts sample perimeter tracings (black lines) with highlighted interfaces of heterotypic contacts corresponding to hepatocytes in a digitally acquired phase micrograph. This particular pattern

($200\ \mu\text{m}/500\ \mu\text{m}$) has very little heterotypic contact as is visually observed; therefore, the average χ over the population is small, due to the majority of cells with $\chi = 0$. In Figure 6 we demonstrated the ability to vary the mean value of χ over a cell population from 0.7 in the randomly distributed culture to 0.08 using micropatterning. Moreover, different patterns (20/50) produce distinct mean values of χ ($\chi = 0.55$). These variations in cellular microenvironment, both in amount and variability, were achieved without varying the numbers of cells in each subpopulation.

DISCUSSION

Traditional co-culture systems have been limited by the inability to vary cell local seeding density independently of the cell number as well as inherent variations in the distribution of cell contacts over a population of cells. We have developed a versatile technique for the micropatterning of two different cell types based on existing strategies for surface modification with aminosilanes linked to biomolecules and the manipula-

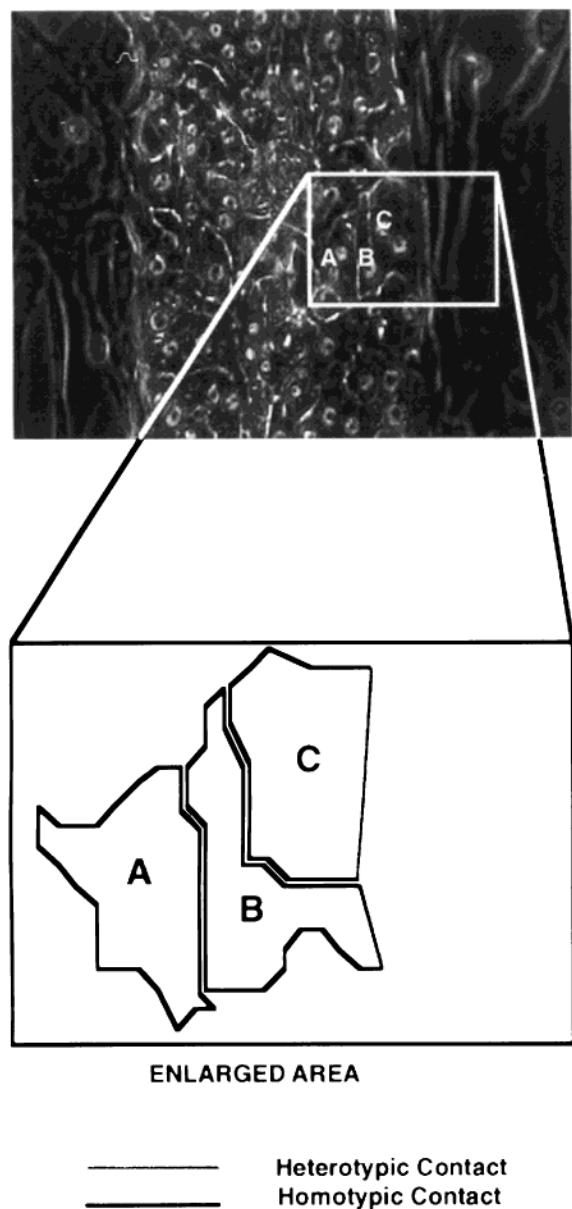


Figure 5. Schematic of method for determining χ , heterotypic interaction parameter. Sample perimeter tracings depicting method for determining heterotypic interaction, χ , for individual cells in digitized images. Solid, black line represents homotypic interaction, H, grey line depicts heterotypic interaction, F. Therefore, $\chi = F/P$ where $P = H + F$.

tion of serum content of cell culture media. This coculture technique allows the manipulation of the initial cellular microenvironment without variation of adhered cell number. Specifically we were able to control both the degree and type of initial cell-cell contact. Differences in homotypic and heterotypic interaction were demonstrated, allowing variations in exposure to cell-surface receptors, locally secreted extracellular matrix, and local concentrations of soluble factors.

Heterotypic Interactions

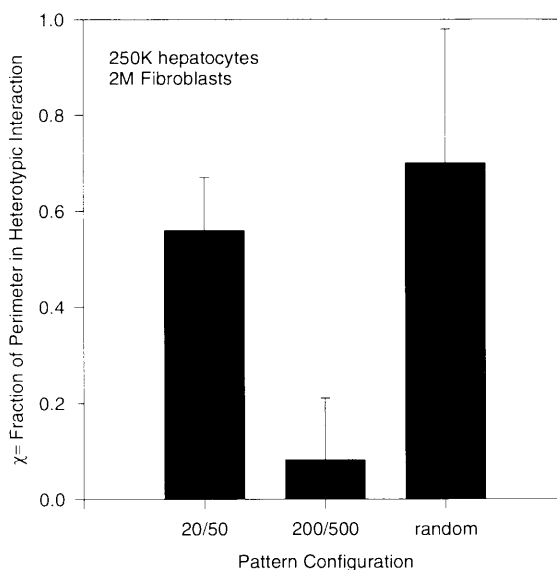


Figure 6. Heterotypic interaction in co-cultures. Average heterotypic interaction, χ , 30 h after hepatocyte seeding, 6 h after fibroblast seeding, in co-cultures containing identical cell numbers; 20/50 represents micropatterns of 20- μm hepatocyte lanes, 50- μm fibroblast lanes, 200/500 represents micropatterns containing 200- μm hepatocyte lane, 500- μm fibroblast lane, and random refers to randomly distributed cocultures. Values of χ are obtained by image analysis for each cell in a digitized image and represents the fraction of hepatocyte perimeter in contact with fibroblasts (see METHODS and Fig. 5).

The patterning methodology utilized in this study represents significant modification of many existing techniques. Specifically, our approach differs from other patterning techniques in the method and timing of surface modification AS. Aminoethylaminopropyltrimethoxysilane was applied after photoresist patterning but before photoresist lift off. This differs from Lom et al.,¹⁹ who apply AS before photoresist application. The microfabrication facility utilized for the manufacture of these substrates, like many others, restricts presence of classes III-V compounds for quality control of semiconductor fabrication; therefore, AS modification of borosilicate cannot be performed prior to photoresist application. In contrast, other groups^{17,39} typically modify exposed glass with alkylsilanes in solvents which do not attack photoresist, such as chlorobenzene. Subsequently, photoresist is lifted off in acetone and AS is deposited in ethanol on newly exposed glass. In these systems incubation with biomolecules, such as horseradish peroxidase, results in adsorption to both regions which becomes specific after denaturation of nonspecifically bound protein in 8M urea. Many proteins, such as collagen, undergo irreversible adsorption⁴⁰ and will therefore not desorb

from unmodified regions. We preserved the integrity of the photoresist throughout the surface-modification process and removed the photoresist after the deposition of collagen. This was achieved by deposition of AS in water, which does not normally attack photoresist. Aminoethylaminopropyltrimethoxysilane is known to oligomerize in aqueous solution,⁴¹ but is stable at least for a period of hours. In this way we utilized photoresist to mask the borosilicate from nonspecific protein adsorption and did not need to rely on protein denaturation and desorption nor on AS deposition prior to photoresist patterning.

Atomic force microscopy was utilized to approximate the depth of the immobilized collagen layer. Modified regions were ~4 nm above the unmodified regions. Aminoethylaminopropyltrimethoxysilane molecules have been estimated to have a height of 1.2¹⁹ nm end to end. In the helical configuration, collagen I fibrils have dimensions of 300 nm in length and 1.2 nm in diameter.⁴² These data suggest that we have only 1–2 layers of collagen fibrils, configured lengthwise, despite the high concentration of collagen solution utilized in the immobilization procedure, corresponding to an upper limit of 0.1 $\mu\text{g}/\text{cm}^2$ per monolayer of “side-on” packed fibrils.⁴⁰ Therefore, achievable collagen-surface concentrations are within an order of magnitude of those observed in adsorbed collagen systems (0.37 $\mu\text{g}/\text{cm}^2$).⁴⁰ Another consideration is the bioactivity of biomolecules after exposure to acetone and ethanol. We have demonstrated preservation of bioactivity of collagen I via cell attachment and spreading as well as by antibody binding for indirect immunofluorescence. Others have shown functional integrity of laminin, fibronectin, collagen IV, and BSA.¹⁹ Proteins sensitive to acetone may require adaptation of the photoresist lift-off procedure.

In the described technique selective cell attachment to immobilized collagen was enhanced by adsorption of BSA to the surface to deter nonspecific adhesion. This has been shown to be effective for hepatocytes, neuroblastoma cells,^{19,29,30} and many antibody–antigen interactions. In contrast albumin adsorption to (mono)aminosilane on fluorinated ethylene propylene films has been shown to have the opposite effect of mediating attachment of aortic endothelial cells²⁰; therefore, this aspect of the procedure may require optimization for generalization to other cell types.

Using primary rat hepatocytes and 3T3 fibroblasts, we demonstrated the ability to vary initial heterotypic (χ) interactions over a wide range while preserving the ratio of cell populations in culture. Thus, co-culture interactions may be manipulated in an entirely new dimension. In addition, micropatterned co-cultures were observed to have less variation in the level heterotypic contacts (χ) than random co-cultures. Therefore, measurement of macroscopic biochemical quantities in micropatterned co-cultures will be better representa-

tions of specific cell–cell interactions than those seen in random co-cultures.

In general, this methodology for micropatterning co-culture also can be applied to other techniques of patterning biomolecules, such as self-assembled monolayers. In addition three-phase co-cultures theoretically can be established by patterning of two different, cell-specific biomolecules. The versatility of the technique is, however, limited by a number of experimental constraints. First, this methodology only allows manipulation of initial culture conditions. Motile and mitotic cells will eventually intermix although the time scale of interest may not exclude meaningful experimentation. We have explored a variety of strategies to prevent this intermixing including cytoskeletal agents (cytochalasins, phalloidin), topological modification of the surface (i.e., seeding cells in grooves), and mitotic agents (mitomycin C). These approaches may be tailored to each culture system to minimize the degree of deviation from the initial pattern.

In summary, we have developed a simple, versatile technique for controlling homotypic versus heterotypic interactions of at least two cell types in culture, by modification of existing micropatterning technologies and utilization of serum-protein adsorption to facilitate cell attachment. This methodology has potential applications in developmental biology,⁴³ tissue engineering, and implant biology both in the arena of basic science and functional optimization.

Many thanks go to Dr. Jim Brown of Cytonix, Inc., and Dr. Prabhas Moghe of Rutgers University. The authors are also grateful to Kealy Ham, William Holmes, Kristin O’Neil, and Annie Tsong for their technical assistance. This work was partially supported by grants from the Shriners Hospital for Crippled Children and from the NIH (DK46270).

References

1. M. F. Fillinger, S. E. O’Connor, R. J. Wagner, and J. L. Cronenvett, “The effect of endothelial cell coculture on smooth muscle cell proliferation,” *J. Vasc. Surg.*, **17**, 1058–1068 (1993).
2. C. Coers and A. L. Woolf (eds.), *The Innervation of Muscle*, C. C. Thomas, Springfield, Illinois, 1959.
3. C. Guguen-Guillouzo, B. Clement, G. Baffet, C. Beaumont, E. Morel-Chany, D. Glaise, and A. Guillouzo, “Maintenance and reversibility of active albumin secretion by adult rat hepatocytes co-cultured with another liver epithelial cell type,” *Exper. Cell Res.*, **143**, 47–54 (1983).
4. P. F. Davies, “Biology of disease: Vascular cell interactions with special reference to the pathogenesis of atherosclerosis,” *Lab Invest.*, **55**, 5–24 (1986).
5. R. Cotran, V. Kumar, and S. Robbins, “Diseases of muscle,” in *Robbins Pathologic Basis of Disease*, R. Cotran, V. Kumar, and S. Robbins (eds.), WB Saunders, PA, 1989, p. 1367.
6. M. J. Olson, M. A. Mancini, M. A. Venkatachalam, and A. K. Roy, “Hepatocyte cytodifferentiation and cell-to-

- cell communication," in *Cell Intercommunication*, W. C. De Mello (ed.), CRC Press, Inc., Boca Raton, Florida, 1990.
7. S. Shimaoka, T. Nakamura, and A. Ichihara, "Stimulation of growth of primary cultured adult rat hepatocytes without growth factors by coculture with nonparenchymal liver cells," *Exper. Cell Res.*, **172**, 228–242 (1987).
 8. F. Goulet, C. Normand, and O. Morin, "Cellular interactions promote tissue-specific function, biomatrix deposition and junctional communication of primary cultured hepatocytes," *Hepatology*, **8**, 1010–1018 (1988).
 9. O. Morin, F. Goulet, and C. Normand, "Liver Sinusoidal Endothelial Cells: Isolation, Purification, Characterization and Interaction with Hepatocytes," *Cell Biology Reviews*, **15**, 2–69 (1988).
 10. M. B. Lawrence, L. V. McIntire, and S. G. Eskin, "Effect of flow on polymorphonuclear leukocyte/endothelial cell adhesion," *Blood*, **70**, 1284–1290 (1987).
 11. M. B. Lawrence, C. W. Smith, S. G. Eskin, and L. V. McIntire, "Effect on venous shear stress on CD18-mediated neutrophil adhesion to cultured endothelium," *Blood*, **75**, 227–237 (1990).
 12. J. A. Hammarback, J. B. McCarthy, S. L. Palm, L. T. Furcht, and P. C. Letourneau, "Growth cone guidance by substrate-bound laminin pathways is correlated with neuron-to-pathway adhesivity," *Development. Biol.*, **126**, 29–39 (1988).
 13. T. Matzuda, K. Inoue, and T. Sugawara, "Development of micropatterning technology for cultured cells," *ASAIO Transactions*, **36**, M559–M562 (1990).
 14. J. M. Corey, B. C. Wheeler, and G. J. Brewer, "Compliance of hippocampal neurons to patterned substrate networks," *J. Neurosci. Res.*, **30**, 300–307 (1991).
 15. S. Rohr, D. M. Schölly, and A. G. Kléber, "Patterned growth of neonatal rat heart cells in culture: Morphological and electrophysiological characterization," *Circ. Res.*, **68**, 114–130 (1991).
 16. S. Britland, E. Perez-Arnaud, P. Clark, B. McGinn, P. Connolly, and G. Moores, "Micropatterning proteins and synthetic peptides on solid supports: A novel application for microelectronics fabrication technology," *Biotechnol. Prog.*, **8**, 155–160 (1992).
 17. D. A. Stenger, J. H. Georger, C. S. Dulcey, J. J. Hickman, A. S. Rudolph, T. B. Nielsen, S. M. McCort, and J. M. Calvert, "Coplanar molecular assemblies of amino- and perfluorinated alkylsilanes: Characterization and geometric definition of mammalian cell adhesion and growth," *J. Am. Chem. Soc.*, **114**, 8435–8442 (1992).
 18. P. Clark, S. Britland, and P. Connolly, "Growth cone guidance and neuron morphology on micropatterned laminin," *J. Cell Sci.*, **105**, 203–212 (1993).
 19. B. Lom, K. E. Healy, and P. E. Hockberger, "A versatile technique for patterning biomolecules onto glass coverslips," *J. Neurosci. Meth.*, **50**, 385–397 (1993).
 20. J. P. Ranieri, R. Bellamkonda, J. Jacob, T. G. Vargo, J. A. Gardella, and P. Aebischer, "Selective neuronal cell attachment to a covalently patterned monoamine on fluorinated ethylene propylene films," *J. Biomed. Mater. Res.*, **27**, 917–925 (1993).
 21. E. T. den Braber, J. E. de Ruijter, H. T. J. Smits, L. A. Ginsel, A. F. von Recum, and J. A. Jansen, "Effect of parallel surface microgrooves and surface energy on cell growth," *J. Biomed. Mater. Res.*, **29**, 511–518 (1995).
 22. J.-S. Lee, M. Kaibara, M. Iwaki, J. Sasabe, Y. Suzuki, and M. Kusakabe, "Selective adhesion and proliferation of cells on ion-implanted polymer domains," *Biomaterials*, **14**, 71–93 (1993).
 23. A. Soekarno, B. Lom, and P. E. Hockberger, "Pathfinding by neuroblastoma cells in culture is directed by preferential adhesion to positively charged surfaces," *NeuroImage*, **1**, 129–144 (1993).
 24. T. Matsuda, T. Sugawara, and K. Inoue, "Two-dimensional cell manipulation technology," *ASAIO J.*, **38**, M243–M247 (1992).
 25. R. Singhvi, G. Stephanopoulos, and D. I. C. Wang, "Review: Effects of substratum morphology on cell physiology," *Biotechnol. Bioeng.*, **43**, 764–771 (1994).
 26. C. Oakley and D. M. Brunette, "Topographic compensation: Guidance and directed locomotion of fibroblasts on grooved micromachined substrata in the absence of microtubules," *Cell Motility Cytoskel.*, **31**, 45–58 (1995).
 27. R. W. Gundersen, "Response of sensory neurites and growth cones to patterned substrata of laminin and fibronectin *in vitro*," *Development. Biol.*, **121**, 423–431 (1987).
 28. R. Singhvi, A. Kumar, G. P. Lopez, G. N. Stephanopoulos, D. I. C. Wang, G. M. Whitesides, and D. E. Ingber, "Engineering cell shape and function," *Science*, **264**, 696–698 (1994).
 29. S. Miyamoto, A. Ohashi, J. Kimura, S. Tobe, and T. Akaike, "A novel approach for toxicity sensing using hepatocytes on a collagen-patterned plate," *Sensors Actuators B*, **13–14**, 196–199 (1993).
 30. S. N. Bhatia, M. Toner, R. G. Tompkins, and M. L. Yarmush, "Selective adhesion of hepatocytes on patterned surfaces," *Ann. NY Acad. Sci.*, **745**, 187–209 (1994).
 31. M. T. Donato, M. J. Gómez-Lechón, and J. V. Castell, "Drug metabolizing enzymes in rat hepatocytes cocultured with cell lines," *In Vitro Cell. Dev. Biol.*, **26**, 1057–1062 (1990).
 32. R. Langenbach, L. Malick, A. Tompa, C. Kuszynski, H. Freed, and E. Huberman, "Maintenance of adult rat hepatocytes on c3H/10T1/2 cells," *Cancer Res.*, **39**, 3509–3514 (1979).
 33. W. Kuri-Harchuch and T. Mendoza-Figueroa, "Cultivation of adult rat hepatocytes on 3T3 cells: Expression of various liver differentiated functions," *Differentiation*, **41**, 148–157 (1989).
 34. O. Morin and C. Normand, "Long-term maintenance of hepatocyte functional activity in co-culture: Requirements for sinusoidal endothelial cells and dexamethasone," *J. Cell. Physiol.*, **129**, 103–110 (1986).
 35. J. C. Y. Dunn, R. G. Tompkins, and M. L. Yarmush, "Long-term in vitro function of adult hepatocytes in a collagen sandwich configuration," *Biotechnol. Prog.*, **7**, 237–245 (1991).
 36. P. O. Seglen, "Preparation of isolated rat liver cells," *Meth. Biol.*, **13**, 29–83 (1976).
 37. J. C. Y. Dunn, M. L. Yarmush, H. G. Koebe, and R. G. Tompkins, "Hepatocyte function and extracellular matrix geometry: Long-term culture in a sandwich configuration," *FASEB J.*, **3**, 174–177 (1989).
 38. J. Lee, J. R. Morgan, R. G. Tompkins, and M. L. Yarmush, "Proline-mediated enhancement of hepatocyte function in a collagen gel sandwich culture configuration," *FASEB J.*, **7**, 586–591 (1993).
 39. D. Kleinfeld, K. H. Kahler, and P. E. Hockberger, "Controlled outgrowth of dissociated neurons on patterned substrates," *J. Neurosci.*, **8**, 4098–4120 (1988).
 40. M. Deyme, A. Baszkin, J. E. Proust, E. Perez, and M. M. Boissonnade, "Collagen at interfaces I. *In situ* collagen

- adsorption at solution/air and solution/polymer interfaces," *J. Biomed. Mater. Res.*, **20**, 951-962 (1986).
41. B. Arkles, J. R. Steinmetz, J. Zazycny, and P. Mehta, "Factors contributing to the stability of alkoxysilanes in aqueous solution," in *Silicon Compounds, Register and Review*, R. Anderson, G. L. Larson, and Craig Smith (eds.), Hüls America, Piscataway, NJ, 1991, pp. 65-73.
 42. J. Darnell, H. Lodish, and D. Baltimore, "The extracellular matrix serves many functions," in *Molecular Cell Biology*, J. Darnell, H. Lodish, and D. Baltimore (eds.), W. H. Freeman and Company, New York, 1990, pp. 904-905.
 43. N. M. Le Douarin, "An experimental analysis of liver development," *Med. Biol.*, **53**, 427-455 (1975).

Received December 6, 1995

Accepted February 27, 1996